

## Radiation-induced crosslinking: II. Effect on the crystalline and amorphous densities of polyethylene\*)

C. J. Chen, D. C. Boose and G. S. Y. Yeh

Departments of Chemical Engineering and Materials Engineering, Macromolecular Research Center, University of Michigan, Ann Arbor, Michigan, USA

*Abstract:* Small-angle x-ray scattering (SAXS) was used to determine the structural changes in polyethylene induced by radiation. The changes in densities of the crystalline and amorphous phases,  $\rho_c$  and  $\rho_a$ , were calculated after direct determination of the mean square density fluctuation  $\langle \eta^2 \rangle$ .  $\rho_a$  increases with increasing radiation dose for both linear and branched polyethylene. This accounts for the serious discrepancy between crystallinities determined from wide-angle x-ray scattering and density measurements. This study confirms our previous proposal that crosslinks occur primarily in the noncrystalline phase, most likely at the defects in the lateral grain boundary regions.

*Key words:* Crosslinking; radiation; polyethylene; density; crystallinity; d-spacings; phase densities; crosslink locations and mechanisms; defects; lateral grain boundaries.

### Introduction

A previous paper [1] reported the results of a study of changes in the crystalline and amorphous densities,  $\rho_c$  and  $\rho_a$ , for a branched polyethylene, BPE (Alathon 10) as a function of radiation dose. The results showed that  $\rho_a$  increased with increasing radiation dose, whereas  $\rho_c$  remained unchanged. It was suggested that crosslinks take place primarily in the non-crystalline phase. In that study, the SAXS intensity was obtained from a microdensitometric tracing of a photograph taken with a pinhole camera. The integrated intensity was approximated as being proportional to the mean-square density fluctuation  $\langle \eta^2 \rangle$  and the volume crystallinity  $v_c$  was approximated by the weight crystallinity  $w_c$ . This paper reports the direct determination of  $\langle \eta^2 \rangle$  from SAXS intensity obtained using slit collimation for samples of both linear and branched polyethylene, as well as the use of derived equations for  $\rho_a$  and  $\rho_c$  that are direct functions of  $\rho$ ,  $w_c$  and  $\langle \eta^2 \rangle$ .

The use of SAXS to determine the densities of the crystalline and amorphous phases of polymers is well

known [2–7]. It has now been demonstrated to be applicable to an irradiated bulk BPE. Among the structural techniques that were used in our earlier study, SAXS intensity measurements were found to be by far the most sensitive in the detection of radiation-induced crosslinking effects. That study was carried out on a branched PE known to consist of small crystallites with substantial lateral grain boundary areas. A question arose if the observed effects were also typical of linear polyethylene, LPE, consisting of larger crystallites and well developed lamellae. A LPE was chosen for the present study, together with another BPE; the same Alathon 10 used primarily for comparative purposes.

### Theoretical background

According to Debye and Bueche [8, 9], and Porod [10], the invariant  $Q$  is defined as

$$Q = \int_0^{\infty} m^2 I(m) dm, \quad (1)$$

\*) Dedicated to Prof. Dr. W. Pechhold on the occasion of his 60th birthday.

where  $I$  is the SAXS intensity obtained from pinhole collimation,  $m = 2a \sin \theta$ , and  $a$  is the distance between the sample and the plane of registration.  $Q$  is independent of the arrangement of scattering units and depends only on the mean-square fluctuation of electron density  $\langle \eta^2 \rangle$ :

$$Q = k P_0 d a \langle \eta^2 \rangle, \quad (2)$$

where  $k = (i_e/2\pi) \lambda^3 N^2 = 0.834 \times 10^{-2}$ .  $i_e$  is Thompson's constant ( $7.9 \times 10^{-26}$ ),  $\lambda$  is the wavelength of the  $CuK\alpha$  peak,  $N$  is Loschmidt's number,  $P_0$  is the primary energy, and  $d$  is the sample thickness.

For a two-phase structure consisting of crystalline and amorphous phases with densities  $\rho_c$  and  $\rho_a$ ,  $\langle \eta^2 \rangle$  is given by [10]

$$\langle \eta^2 \rangle = v_c v_a (\rho_c - \rho_a)^2, \quad (3)$$

where  $v_c$  and  $v_a$  are the respective volume fractions. The density difference ( $\rho_c - \rho_a$ ) or  $\Delta\rho$  can be obtained from  $\langle \eta^2 \rangle$  if the volume fractions are known.

In order to determine the crystalline and amorphous densities,  $\rho_c$  and  $\rho_a$ , another relation is required:

$$v_c = (\rho - \rho_a) / (\rho_c - \rho_a) = (\rho / \rho_c) w_c. \quad (4)$$

Using weight crystallinity  $w_c$  from WAXS,  $\langle \eta^2 \rangle$  from SAXS, and the experimentally measured bulk density  $\rho$ , the values of  $\rho_c$  and  $\rho_a$  can be obtained according to the following derived equations from Eqs. (3) and (4):

$$\rho_c = \rho + \frac{\langle \eta^2 \rangle}{2\rho w_c} + \left\{ \frac{\langle \eta^2 \rangle}{w_c} \left[ (1 - w_c) + \frac{\langle \eta^2 \rangle}{4\rho^2 w_c} \right] \right\}^{1/2} \quad (5)$$

$$\rho_a = \rho + \frac{\langle \eta^2 \rangle}{2\rho(1 - w_c)} - \left\{ \frac{\langle \eta^2 \rangle}{(1 - w_c)} \left[ w_c + \frac{\langle \eta^2 \rangle}{4\rho^2(1 - w_c)} \right] \right\}^{1/2}. \quad (6)$$

These equations are different from those used by others [4, 7], where they expressed  $\rho_c$  and  $\rho_a$  in terms of  $v_c$  (then approximated by  $w_c$ ), rather than  $w_c$ ; their equations are relatively straight forward to derive.

## Experimental

Two kinds of polyethylene, a BPE Alathon 10 and a LPE Alathon 7040, were used in our experiments. The Alathon 10 samples were the same ones used in a previous study [1]. The BPE has a density of  $0.92 \text{ g/cm}^3$  and a viscosity average molecular weight  $M_v$  of 52 200. Alathon 7040 has a density of  $0.95 \text{ g/cm}^3$  and a  $M_v$  of 41 500. Sample preparations and irradiation methods have been described in the previous paper [1], along with procedures for gelation, density and WAXS measurements. Radiation doses range from 10 to 400 Mrad.

SAXS was conducted on a Rikagu-Denki camera with Ni-filtered  $CuK\alpha$  radiation and slit collimation. Intensities were recorded with a proportional counter in connection with a pulse height discriminator. Step scans from 0.1 to 3.0 degrees ( $2\theta$ ) in increments of 0.05 degrees were made with intensity recorded by measuring the time per 5 000 counts. This results in a probable counting error of less than 1 % for each measurement [11]. The smeared SAXS intensity was corrected for slit length using Schmidt's program [12].

## Results

Gel content increases with increasing radiation dose, shown in Fig. 1, for both Alathon 10 and Alathon 7040, indicating the formation of a network structure in the irradiated samples. Also shown in Figure 1 are plots of  $1/M_c$  against radiation dose.  $M_c$  is the average molecular weight between crosslinks calculated from Flory-Huggins' equation [13]. Straight lines are obtained for both materials, indicating that the crosslink density is linearly proportional to the radiation dose in the range studied.

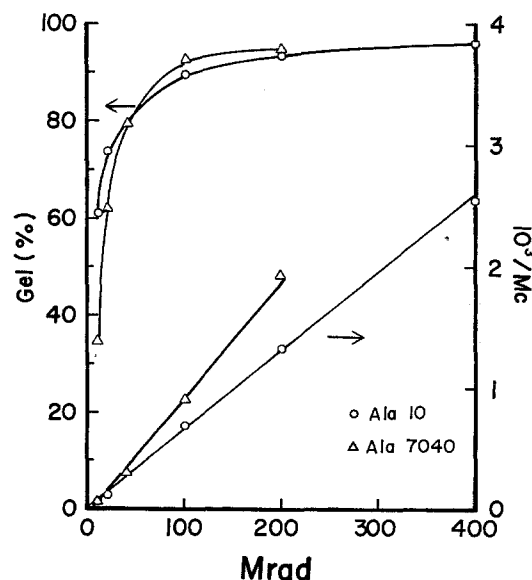


Fig. 1. Changes in gel content and  $1/M_c$  as a function of radiation dose for BPE Alathon 10 and LPE Alathon 7040

Figure 2 shows changes in the bulk density with increasing radiation doses. Density increases slightly with increasing dose for both polyethylenes. Values of volume crystallinity  $v_c$  calculated from these density data, using the conventional constant values of  $\rho_c$  and  $\rho_a$ , are shown by dotted lines in Fig. 3.

Using these constant values, crystallinity appears to increase slightly with radiation. In contrast,  $w_c$  determined from WAXS, plotted in solid lines in Fig. 3, shows a decrease, as generally expected for crosslinked polyethylene with increasing radiation. A similar crystallinity decrease with increasing radiation dose has also been observed from heat of fusion measurements [14]. These noticeable discrepancies can be resolved as we had done previously [1] by using crystalline  $\rho_c$  and amorphous  $\rho_a$  density values that have been corrected for the effects of radiation.

A typical slit-smear SAXS curve is shown in Fig. 4 with error bars included. Collimation corrections for finite slit length were made using Schmidt's program [12]. Figure 5 shows both the slit-smear and the corrected SAXS curves for unirradiated Alathon 10. The correction not only sharpens the peak, but shifts its position toward a higher angle. The long periods calculated from peak positions are 220 Å and

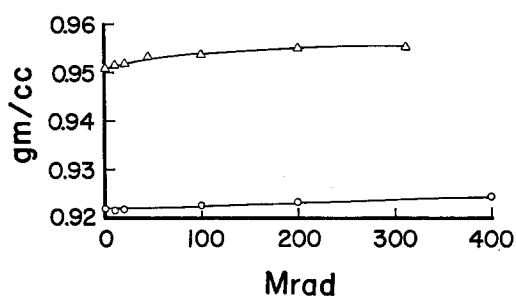


Fig. 2. Changes in density as a function of radiation dose for Alathon 10 (○) and 7040 (△)

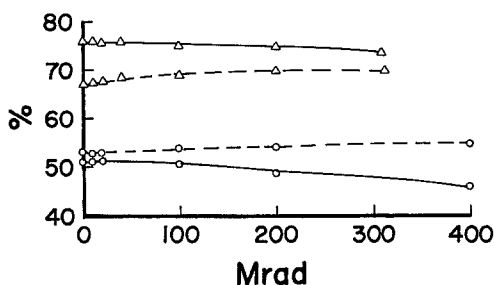


Fig. 3. Changes in crystallinities as a function of radiation dose for Alathon 10 (○) and 7040 (△). Solid lines represent  $w_c$  (from WAXS) and dotted lines represent  $v_c$  (from density).

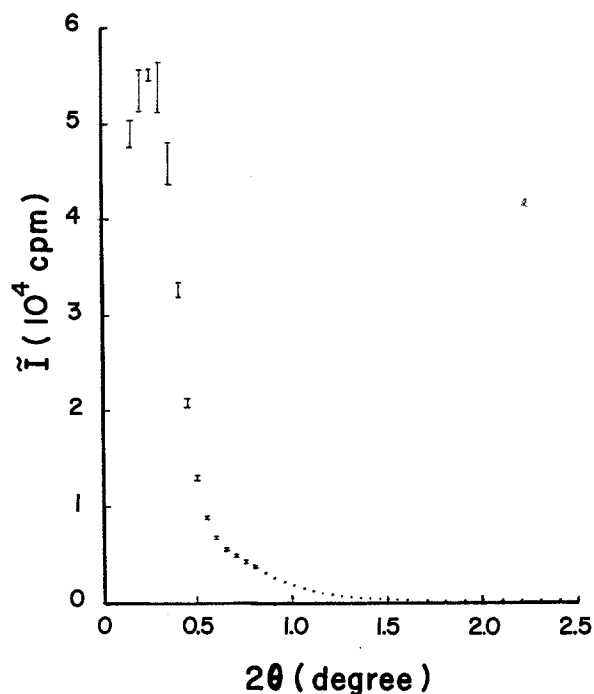


Fig. 4. Typical smeared SAXS curve for PE. Error bars are included.

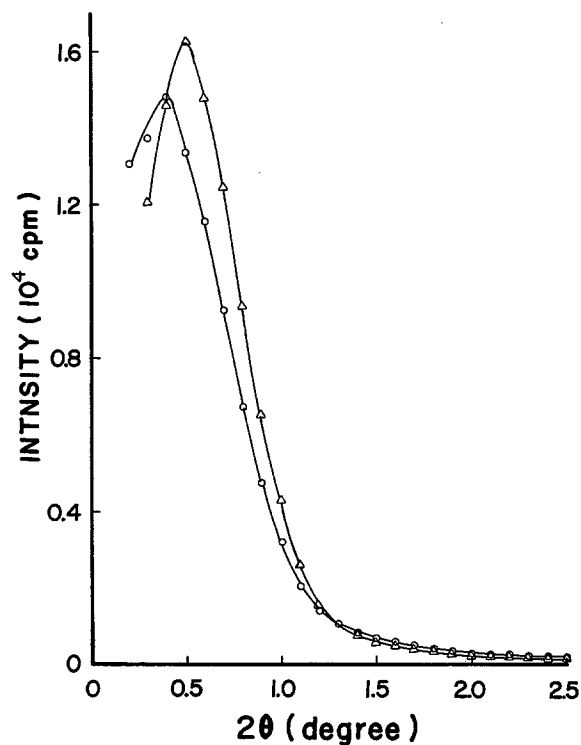


Fig. 5. SAXS curves of an unirradiated Alathon 10. Slit-smear (○) and desmeared (△)

170 Å for smeared and corrected Alathon 10, respectively. For Alathon 7040 the corresponding values are 325 Å and 275 Å.

The slit-smeared SAXS curves of Alathon 10 and Alathon 7040 for various radiation doses are shown in Figs. 6 and 7. The peak intensity decreases with increasing radiation while the peak position remains unchanged, the latter indicating that the long period remains essentially constant with increasing degrees of crosslinking.

The SAXS intensity, corrected for finite slit length, was used to determine the invariant  $Q$  according to Eq. (1). By partial integration we have

$$Q = \int_0^{\infty} m^2 I(m) dm = \int_0^{m^*} m^2 I(m) dm + \int_{m^*}^{\infty} m^2 I(m) dm. \quad (7)$$

The first part of the integral measures the area under the curve  $m^2 I(m)$  vs  $m$  from 0 to  $m^*$  ( $m^*$  was 1.248 cm for this study). This area contributes 85–90% of the total  $Q$  value for all samples. (The contribution of the unobserved part of the scattering curve at the smallest angles was estimated by extrapolating the  $m^2 I(m)$  curve down to  $m = 0$ .) Using the relation  $I(m) \propto m^4$  for the tail of the scattering curve (derived

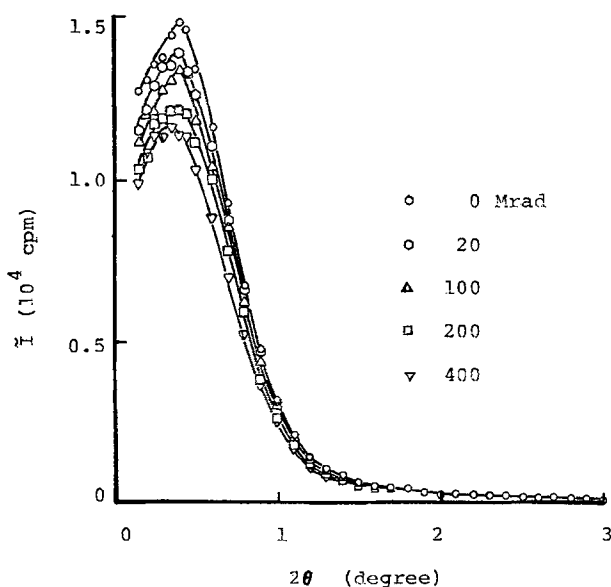


Fig. 6. SAXS curves of Alathon 10 with various radiation doses

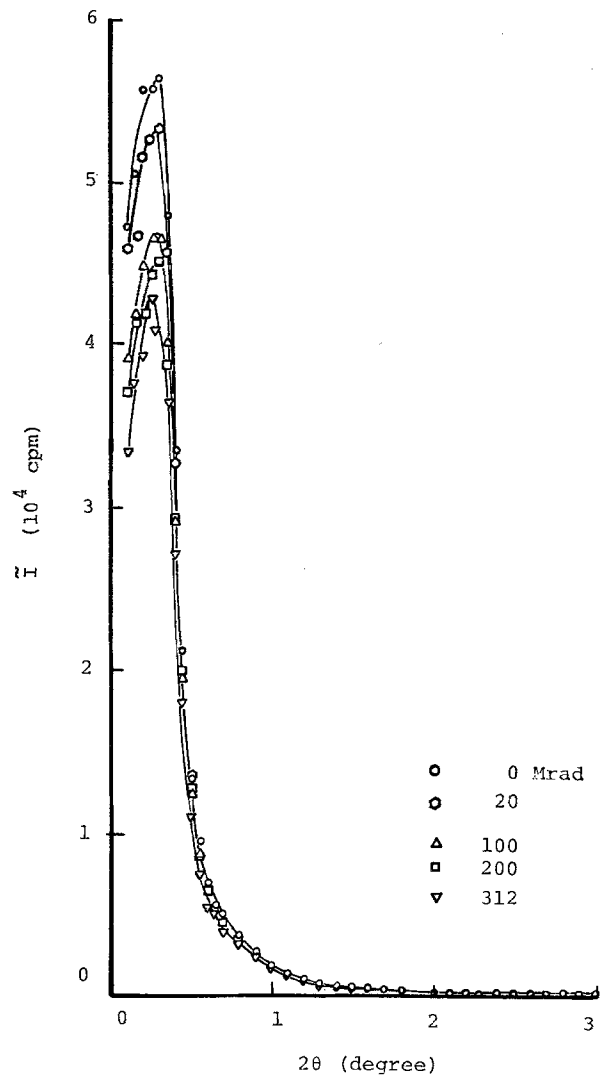


Fig. 7. SAXS curves of Alathon 7040 with various radiation doses

from Porod's theory [10]) the second integral becomes

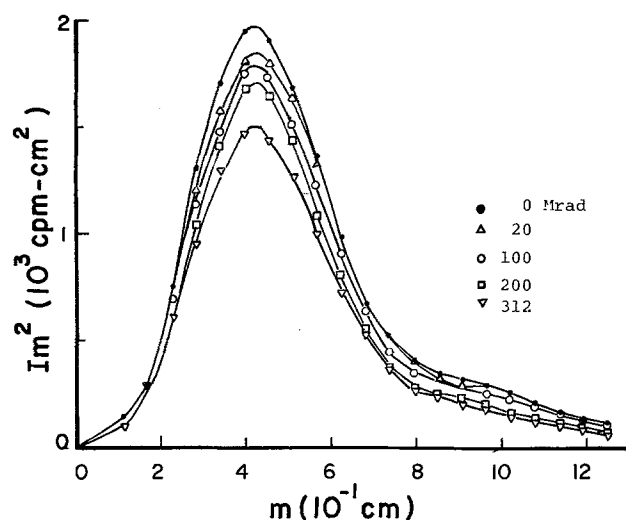
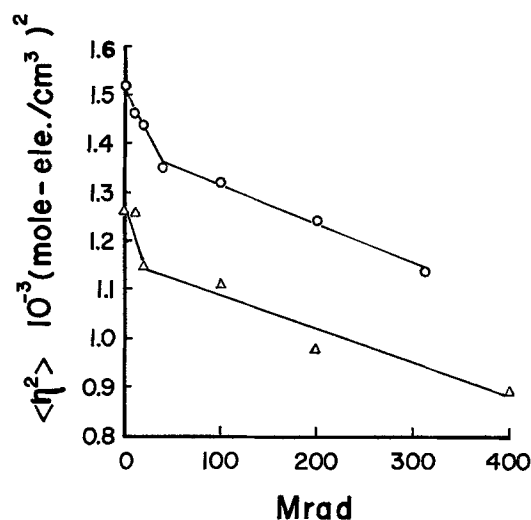
$$\int_{m^*}^{\infty} m^2 I(m) dm = \int_{m^*}^{\infty} m^2 (c/m)^4 dm = c/m^*, \quad (8)$$

where  $c$  is the intercept of a  $m^4 I(m)$  versus  $m^4$  plot. The errors introduced by these simplifications are believed to be less than 10% [4]. Figure 8 shows plots of  $m^2 I(m)$  vs  $m$  for BPE Alathon 10 samples.

Table 1 lists the  $Q$  values of both polymers for various radiation doses.  $Q$  is observed to decrease with increasing radiation, indicating a decrease in mean-square density fluctuation  $\langle \eta^2 \rangle$  with dose

Table 1.

Sample	Mrad	0	10	20	40	100	200	312	400
Alathon 10	$Q(\text{cpm}\cdot\text{cm}^3) \langle \eta^2 \rangle \times 10^3$	1013.69	1011.43	920.75	—	893.20	783.19	—	718.06
	$(\text{mole}\cdot\text{elec}/\text{cm}^3)^2$	1.260	1.257	1.145	—	1.110	0.974	—	0.893
Alathon 7040	$Q(\text{cpm}\cdot\text{cm}^3) \langle \eta^2 \rangle \times 10^3$	1220.64	1176.90	1157.35	1087.19	1061.87	1000.91	914.00	—
	$(\text{mole}\cdot\text{elec}/\text{cm}^3)^2$	1.517	1.463	1.439	1.351	1.320	1.244	1.136	—

Fig. 8.  $m^2 I(m)$  vs  $m$  plots for Alathon 10 of various doses.Fig. 9. Changes in mean-square density fluctuation as a function of radiation dose for Alathon 10 ( $\Delta$ ) and 7040 ( $\circ$ ).

since  $Q$  depends only on  $\langle \eta^2 \rangle$  (see Eq. (2)). The decrease in  $\langle \eta^2 \rangle$  amounts to 25–30 % of the initial values at 300–400 Mrad, as shown in Fig. 9 and Table 1.  $\langle \eta^2 \rangle$  was obtained in absolute units (mole-electrons/ $\text{cm}^3$ )<sup>2</sup> using a calibrated Kratky sample. The  $\langle \eta^2 \rangle$  values are  $1.260 \times 10^{-3}$  and  $1.517 \times 10^{-3}$  for unirradiated branched and linear PE, respectively. These values are in excellent agreement with reported values [4, 15], being between  $1.0 \times 10^{-3}$  and  $1.88 \times 10^{-3}$ .

The densities of the crystalline and amorphous phases,  $\rho_c$  and  $\rho_a$  (Fig. 10) were calculated from Eqs. (5) and (6) using  $w_c$  from WAXS,  $\langle \eta^2 \rangle$  from SAXS and  $\rho$  from density gradient column measurements. Values of  $\rho_c$  and  $\rho_a$  are also listed with density, crystallinity, and  $\langle \eta^2 \rangle$  values in Tables 2 and 3 for Alathon 10 and Alathon 7040, respectively.

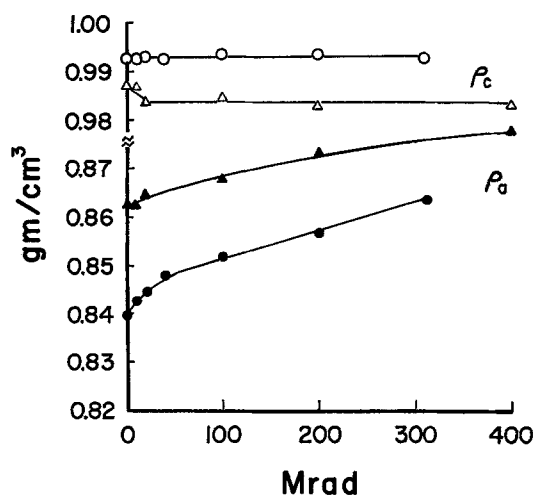
Fig. 10. Changes in crystalline and amorphous densities as a function of radiation dose for Alathon 10 ( $\Delta$  and  $\blacktriangle$ ) and 7040 ( $\circ$  and  $\bullet$ ).

Table 2.

Mrad	$\rho(\text{g}/\text{cm}^3)$	$w_c(\%)$	$\langle \eta^2 \rangle \times 10^3$ (mole- elec/ $\text{cm}^3$ ) <sup>2</sup>	$\rho_c(\text{g}/\text{cm}^3)$	$\rho_a(\text{g}/\text{cm}^3)$
0	0.9218	50.94	1.260	0.987	0.863
10	0.9216	50.89	1.257	0.987	0.863
20	0.9215	51.17	1.145	0.983	0.865
100	0.9226	50.30	1.110	0.984	0.868
200	0.9230	48.52	0.974	0.983	0.873
400	0.9241	46.96	0.893	0.983	0.878

Table 3.

Mrad	$\rho(\text{g}/\text{cm}^3)$	$w_c(\%)$	$\langle \eta^2 \rangle \times 10^3$ (mole- elec/ $\text{cm}^3$ ) <sup>2</sup>	$\rho_c(\text{g}/\text{cm}^3)$	$\rho_a(\text{g}/\text{cm}^3)$
0	0.9508	75.94	1.517	0.993	0.840
10	0.9514	75.74	1.463	0.993	0.843
20	0.9517	75.41	1.439	0.993	0.845
40	0.9530	75.77	1.351	0.992	0.848
100	0.9536	74.94	1.320	0.993	0.852
200	0.9548	74.68	1.244	0.994	0.856
312	0.9549	73.55	1.136	0.993	0.863

$\rho_c$  remains essentially constant for both polymers, i.e.,  $0.983 \text{ g}/\text{cm}^3$  for Alathon 10 and  $0.993 \text{ g}/\text{cm}^3$  for Alathon 7040. There appears to be a small decrease in  $\rho_c$  at small doses for the BPE, though the magnitude of decrease is within the experimental error. In contrast, the amorphous density  $\rho_a$  increases continuously with increasing radiation dose, from  $0.863 \text{ g}/\text{cm}^3$  to  $0.878 \text{ g}/\text{cm}^3$  for branched PE and from  $0.840$  to  $0.863 \text{ g}/\text{cm}^3$  for linear PE. These results are in agreement with previous results on Alathon 10 obtained by photographic methods [1].

## Discussion

Again, one significant result from this study is the demonstration of SAXS for determining the structural changes induced by irradiation of PE. Interestingly, the changes can be seen in both LPE and BPE.

The mean-square density fluctuation  $\langle \eta^2 \rangle$  decreases by 25–30 % of its original value with 300–400 Mrad. This reduction is much greater than the

estimated maximum experimental error of 10 %. Even for a dose of 100 Mrad there is a 12 % decrease in  $\langle \eta^2 \rangle$ . In comparison, WAXS, the most commonly used technique for structural determinations, cannot detect a significant change in that dose range. For example, crystallinity determined from WAXS remains almost constant up to 100 Mrad. We now consider in greater detail the various origins for the observed decrease in  $\langle \eta^2 \rangle$ .

The lamellar structure of polymers is usually described as having a simple two-phase morphology, with crystalline and amorphous densities  $\rho_c$  and  $\rho_a$  considered constant, and having a sharply defined boundary between the phases. This simple model has been shown to adequately describe PE both crystallized from solution [2, 15] and from the melt [4, 15], but has been shown to be invalid for drawn PE [5] and for PET [7] (both drawn and undrawn). The validity of such a two-phase model with respect to irradiated PE may be checked by comparing the experimentally determined values of the mean-square density fluctuation  $\langle \eta^2 \rangle_{\text{exp}}$ , taken from  $Q$  values (by Eq. 2), with values calculated assuming a two-phase model with constant  $\rho_c$  and  $\rho_a$  densities:

$$\langle \eta^2 \rangle_{\text{cal}} = v_c v_a (\rho_c - \rho_a)^2. \quad (9)$$

The ratio of these two values,  $\langle \eta^2 \rangle_{\text{exp}} / \langle \eta^2 \rangle_{\text{cal}}$ , should be approximately equal to 1 if the model is valid. A plot of these ratios as a function of radiation dose, shown in Fig. 11, reveals that the simple two-phase

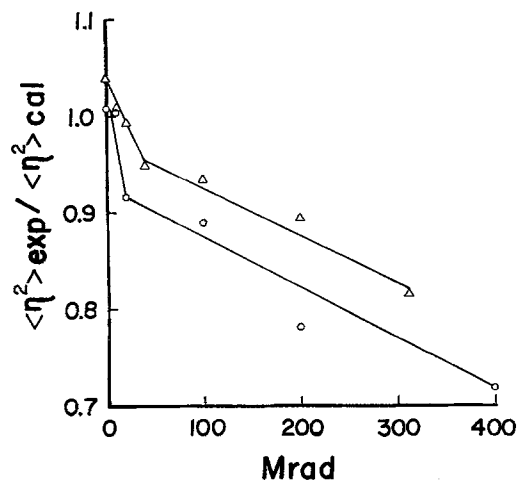


Fig. 11. Changes in the ratio of experimental to calculated mean square density fluctuations as a function of radiation dose for Alathon 10 ( $\circ$ ) and 7040 ( $\triangle$ ).

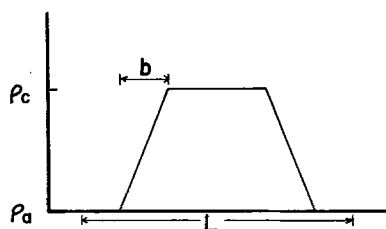


Fig. 12. Schematic representation of electron density distribution with a finite length of transition zone.

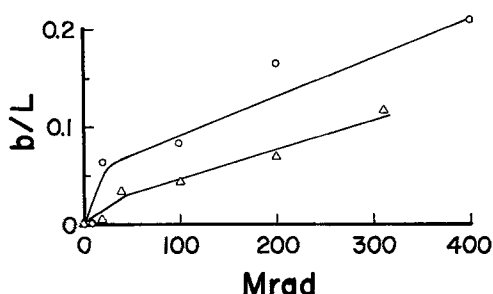


Fig. 13. Dependence of the ratio  $b/L$  on radiation dose for Alathon 10 (O) and 7040 ( $\Delta$ ).

model is a fair approximation for unirradiated PE, but the model is increasingly in error as the radiation dose increases. Thus, the structure of irradiated PE cannot be described by the ideal two-phase model, as had already been implied in our previous study [1], as well as by the demonstration [1] that corrected  $\rho_c$  and  $\rho_a$  values must be used in order to obtain correct values of  $v_c$ .

The inadequacy of the simple two-phase model for irradiated PE may also imply that a transition region of finite width exists between the crystalline and amorphous phases.

For a system having a transition zone with a linear density gradient, as shown schematically in Fig. 12, Eq. (3) can be modified as follows [16, 17]:

$$\langle \eta^2 \rangle = (\rho_c - \rho_a)^2 [v_a v_c - b/(3L)], \quad (10)$$

where  $b$  is the width of the transition zone and  $L$  is the long period. The ratio  $b/L$  can be calculated from the experimental value of  $\langle \eta^2 \rangle$  and volume fraction  $v_c$ , using the conventional values of  $\rho_c$  and  $\rho_a$ . The ratio  $b/L$ , plotted in Fig. 13, shows an increase with increasing radiation for both polymers, from about 0 (at 0 Mrad) to 0.21 at 400 Mrad for Alathon 10 and to 0.12 at 312 Mrad for Alathon 7040. These values correspond to a transition zone with a width of 36 Å

for Alathon 10 ( $L = 170$  Å) and 32 Å for Alathon 7040 ( $L = 275$  Å).

This increase in the width of the transition zone with radiation could be attributed to crosslinks occurring in the boundaries between the crystalline and amorphous lamellae. If so, the increase in the transition width by 36 Å at 400 Mrad would cause a decrease in crystallinity to 20 %, assuming only half of the transition width contributes to a decrease of chain length in the crystalline phase. This value is much greater than the observed 4 % decrease in crystallinity. Therefore, this type of transition model is not applicable for crosslinked polyethylene and we may assume the existence of a sharp transition, or at least a constant transition width in the irradiated samples. Consequently, the decrease in  $\langle \eta^2 \rangle$  can only be attributed to a decrease in the density difference between phases, suggesting a decrease in  $\rho_c$  and/or an increase in  $\rho_a$ . This led to our reported values of  $\rho_c$  and  $\rho_a$  in the Results Section. Furthermore, changes in the crystalline and amorphous densities can remove the discrepancy between the crystallinities determined from WAXS and density data, which strongly supports the contention that the decrease in  $\langle \eta^2 \rangle$  is basically  $\Delta\rho$  in origin.

The crystalline density  $\rho_c$  remains essentially constant for linear and branched PE, at a value slightly lower than the ideal value (0.993 and 0.983 compared to 0.998), suggesting the presence of defects in the original crystal structure, especially for the BPE. In contrast, the amorphous density  $\rho_a$  increases with increasing radiation. The observed increase in  $\rho_a$  with radiation suggests that crosslinks occur primarily outside the crystals in the amorphous phase. Crosslinks within the crystals would cause defects, leading to a continuous decrease in  $\rho_c$  that is not observed in either BPE or LPE. The present findings give additional confirmation to our previous results on Alathon 10 obtained by photographic methods, as well as the conclusions reached there.

## Conclusions

The use of SAXS to determine the structural changes in PE caused by radiation-induced crosslinking was confirmed. The crystalline density remains essentially unchanged, whereas the amorphous density increases with increasing radiation dose for both branched and linear PE. These results indicate that a simple two-phase model, assuming constant  $\rho_c$  and

$\rho_{cr}$  is not valid for the crosslinked PE. The results also explain the discrepancy between crystallinities determined from WAXS and density measurements. The constant values of crystalline density suggests no crosslinks form within crystals; crosslinking takes place primarily in a non-crystalline phase.

#### Acknowledgement

The authors wish to thank the Macromolecular Research Center and the National Science Foundation for financial support.

#### References

1. Yeh GSY, Chen CJ, Boose DC (1985) *Colloid & Polymer Sci* 263:109
2. Fischer EW, Goddar H, Schmidt GF (1967) *J Polym Sci B5*:619
3. Vonk CG, Kortleve G (1967) *Kolloid Z Polym* 220:19
4. Kortleve G, Vonk CG (1968) *Kolloid Z Polym* 225:124
5. Fischer EW, Goddar H, Schmidt GF (1969) *J Polym Sci A2*, I, 37
6. Kavesh S, Schultz JM (1971) *J Polym Sci A2*, 9:85
7. Fischer EW, Fakirov S (1976) *J Mater Sci* 11:1041
8. Debye P, Bueche A (1949) *J Appl Phys* 20:518
9. Debye P, Anderson HR, Bueche A (1957) *J Appl Phys* 28:679
10. Porod G (1951) *Kolloid Z* 124:83
11. Cullity BD (1967) *Elements of X-Ray Diffraction*, Addison-Wesley, Mass
12. Schmidt PW (1965) *Acta Cryst* 19:938
13. Flory PJ *Principles of Polymer Chemistry*, Cornell Univ Press, New York
14. Chen CJ, unpublished
15. Schmidt PW (1965) *Acta Cryst* 19:938
16. Strobl GR, Muller N (1973) *Polym Sci Phys* 11:1219
17. Tsvankin DY (1964) *Polym Sci USSR* 6:2304-2310

Received May 8, 1990  
accepted July 4, 1990

#### Authors' address:

G. S. Y. Yeh  
Departments of Chemical Engineering and Materials  
Engineering  
Macromolecular Research Center  
University of Michigan  
Ann Arbor, Michigan 48109, USA